

DOI: 10.1002/cctc.201300185

High-Temperature Sulfur Removal from Biomass-Derived Synthesis Gas over Bifunctional Molybdenum Catalysts

Christian F. J. König,^[a] Patrick Schuh,^[a, b] Tilman J. Schildhauer,^[a] and Maarten Nachtegaal^{*[a]}

The removal of sulfur species from the biomass-derived producer gas after gasification is required to protect downstream catalysts. Finding suitable materials for high-temperature desulfurization is one of the main challenges for the improvement in the efficiency of catalytic biomass conversion. The biomass-derived producer gas usually contains not only H₂S but also organic sulfur species such as thiophene (C₄H₄S), which cannot be removed by most sorbent materials. Herein, we explored Al₂O₃-supported molybdenum catalysts as bifunctional materials for the removal of H₂S and catalytic conversion of C₄H₄S at high temperatures. By using X-ray absorption spec-

troscopy under reaction conditions, we show that H₂S is removed through the sulfidation of MoO₃. C₄H₄S is catalytically converted over MoO₂ to MoS₂ and hydrocarbon species. The subsequent oxidation of MoS₂ to MoO₃ and SO₂ regenerates the material and allows the sequestration of sulfur from the gas stream. Furthermore, the negative effect of steam on sulfur removal is shown to be caused by competitive adsorption with sulfur species. These findings show the possibility of the high-temperature desulfurization of biomass-derived gas for catalytic conversion, for instance, to synthetic natural gas.

Introduction

In recent years, biomass has received increased interest as a chemical feedstock or as fuel. Technologies for the thermochemical conversion of biomass to fuels, for example, through gasification, have the potential to be cost competitive with gasoline.^[1]

During gasification of biomass feedstocks, a gas mixture mainly of CO, H₂, CO₂, CH₄, and H₂O is generated.^[2] In addition, depending on gasification parameters, several undesired by-products and contaminants with different concentrations are produced, which include olefins, tars, sulfur, and nitrogen heteroatom species (thiophene [C₄H₄S] and pyridine); inorganic constituents such as sulfur, chlorine, and nitrogen (H₂S, COS, HCl, NH₃, and HCN); and alkali metals.^[3–5] Sulfur-containing compounds are corrosive to pipelines and downstream installations and thus limit plant lifetime.^[6,7] Moreover, sulfur species poison downstream catalysts, which negatively affects the catalyst performance. For example, small amounts of H₂S poison the nickel or ruthenium catalysts used for methanation,^[8,9] hot gas cleaning,^[10] and Fischer–Tropsch synthesis.^[11]

In coal or biomass gasification process chains, sulfur components are often removed by using low-temperature processes (e.g., scrubbing), such as cooling the producer gas from 850 °C (gasification temperature) to below the dew point of H₂O. Reheating up to 250–400 °C for downstream fuel catalysis, neces-

sary re-evaporation of H₂O for the adjustment of the H₂ to CO ratio via steam reforming, and regeneration of scrubbing liquids make cold gas cleaning thermally inefficient and expensive. Technoeconomic analysis showed that processes such as tar reforming and acid gas and sulfur removal comprise up to 31% of the minimum selling price for ethanol produced from biomass.^[12] This finding suggests that efficient sulfur and tar removal can lower costs significantly.

Hot gas desulfurization operating between 300 and 850 °C is preferred to improve the efficiency of biomass-to-fuel conversion.^[13,14] Desulfurization over sorbent materials and/or catalysts leads to the accumulation of sulfur on the sorbent over time on stream. To maintain operation, the sorbent needs to be replaced or regenerated: the latter either periodically (e.g., in a swing reactor) or continuously. For the continuous removal of sulfur from the gas stream, a chemical looping process is used.^[15] For regeneration, the sorbent is exposed to an oxidizing atmosphere, which leads to the production of SO₂, which in turn can be sequestered from the cleaned fuel gas stream. The sequestered SO₂ can then be captured in scrubbers by a slurry or solid sorption materials.^[16,17]

One major challenge for hot gas desulfurization is the identification of materials that remove different sulfur species from the gas in the presence of steam, and that are stable over many cycles of sulfur uptake and regeneration. Zinc titanate sorbents were proposed as regenerable, attrition-resistant H₂S sorbents.^[18] The literature focuses largely on the removal of H₂S from coal gas without investigating organic sulfur compounds.^[19,20] Such organic sulfur compounds are usually present in gasified biomass owing to the low gasification temperature (compared to the temperature of coal gasification) and are not usually removed by sorbents.^[5]

[a] C. F. J. König, P. Schuh, Dr. T. J. Schildhauer, Dr. M. Nachtegaal
Paul Scherrer Institut
5232 Villigen PSI (Switzerland)
Fax: (+41) 56-310-2199
E-mail: maarten.nachtegaal@psi.ch

[b] P. Schuh
Technische Universität München
05747 Garching (Germany)

Molybdenum, along with Ni, Co, or other promoters, removes sulfur-containing components in the hydrodesulfurization (HDS) process in petroleum refining.^[21] In contrast to the HDS process, water vapor is always present in the producer gas from the gasified biomass, either from the moist feedstock or from steam used as a gasification medium.^[22] The competitive adsorption of H₂O on the catalyst has been reported to reduce the desulfurization of C₄H₄S over Co–Mo catalysts,^[23] in hydrodeoxygenation (HDO) over Ni–Mo^[24] and Co–Mo,^[25] and in H₂S removal over ZnO.^[26] Furthermore, the partial pressure of H₂ in the producer gas from atmospheric gasifiers is of the order of several 100 mbar whereas HDS reactors usually operate at a H₂ partial pressure of greater than 10 bar (1 bar = 0.1 MPa).^[21] As the biomass-derived synthesis gas has low partial pressures of H₂ and high amounts of steam, the development of specific materials for the high-temperature desulfurization of biomass-derived synthesis gas is required. Sulfide catalysts, as they are usually used in the HDS process under high H₂ partial pressures, cannot be used for the hot gas desulfurization of biomass with continuous regeneration, because the sulfur on the catalyst would be immediately oxidized to SO₂ upon regeneration.

The sulfidation of Mo catalysts and their HDS activity were studied in the past with various techniques, and the findings are summarized in reviews.^[27,28] The Mo-based catalysts for HDS are usually regarded as slabs of MoS₂, which are terminated by sulfur and eventually doped with Co on the edges of the slab.^[29] The active sites are assumed to be vacancies on the edges of MoS₂. Furthermore, in HDS processes, C₄H₄S is continuously converted to H₂S, which is eliminated downstream in a ZnO bed,^[21] whereas in hot gas desulfurization processes, all sulfur is ideally converted to SO₂ and sequestered from the synthesis gas stream.

Herein, we investigate mechanisms of sulfur removal in a cyclic process from gasified biomass at high temperatures. The goal is to develop a high-temperature gas cleaning process and to understand the mechanisms of removal not only of H₂S but also of organic sulfur species, which are rarely considered in high-temperature gas cleaning studies. As Mo-based catalysts are often used for the conversion of organic sulfur species, Mo is a promising material to accomplish sulfur removal. However, the cyclic operation of sulfur removal and regeneration leads to requirements for the material that are different from those for HDS, which is usually performed at lower temperatures, at much higher H₂ partial pressures, and with

significantly lower steam content. To study the state of Mo under reaction conditions, in situ X-ray absorption spectroscopy (XAS) was used. Recent advances in synchrotron instrumentation are able to perform in situ studies on time scales of seconds or subseconds, which are relevant for dynamic processes, such as chemical looping.^[30] The mechanism of the removal of H₂S was found to be the concurrent sulfidation of MoO₃ to MoS₂ and reduction to MoO₂. The removal of C₄H₄S proceeds via the desulfurization of the C₄H₄S ring, which leads to the sulfidation of MoO₂.

Results

Characterization of the fresh catalyst

To characterize the local structure of the fresh, calcined catalyst, the sample was investigated by using XAS. The X-ray absorption near-edge spectroscopy (XANES) spectra of the fresh Mo/Al₂O₃ catalyst along with the spectra of reference compounds are shown in Figure 1a. The XANES spectra of the

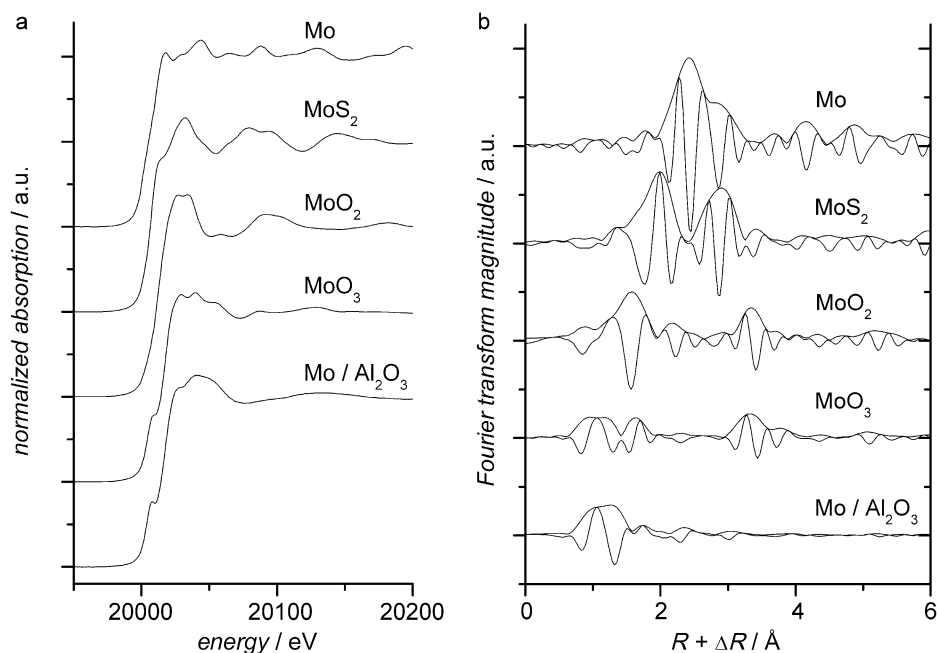


Figure 1. a) Mo K-edge XANES spectra and b) Fourier transforms of the EXAFS spectra of the fresh Mo/Al₂O₃ catalyst sample versus Mo reference compounds for MoO₃, MoO₂, MoS₂, and Mo foil.

fresh catalyst demonstrate features that are similar to those of the reference MoO₃ spectrum, such as the shoulder in the spectrum at 20005 eV and the position of the absorption edge. This qualitative comparison suggests that the fresh Mo catalyst is oxidized to MoO₃ after calcination. The corresponding Fourier transforms of the extended X-ray absorption fine structure (EXAFS) spectra are shown in Figure 1b. In the Fourier transforms, the fresh catalyst shows one peak at approximately 1.2 Å but no significant peaks at higher distances. Based on the comparison to the Fourier transforms of the references, this peak is a Mo–O scattering shell at a distance simi-

lar to that in the MoO₃ reference spectra. According to the XANES and EXAFS spectra, the spectrum of the fresh catalyst is identified as MoO₃. In contrast to the reference spectra, the fresh, calcined MoO₃/Al₂O₃ sample does not show scattering shells at higher distances (such as the Mo–Mo scattering shell at ≈ 1.8 Å), which suggests a small particle size.

Fitting the EXAFS spectrum of the fresh catalyst with a MoO₃ reference structure^[31] yields a coordination number of 3.7 ± 0.5 for the Mo–O shell at a distance of (1.71 ± 0.01) Å, with a Debye–Waller factor of (0.005 ± 0.001) Å². No scattering shells at higher distances could be fitted. The scanning TEM (STEM) analysis of the fresh MoO₃/Al₂O₃ catalyst (Figure 2) re-

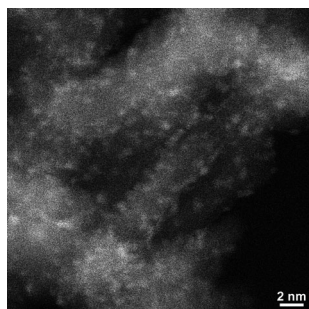


Figure 2. STEM micrograph of the fresh Mo/Al₂O₃ catalyst as measured in the Z-contrast mode.

veals a particle size of approximately 1 nm, which supports the findings of the EXAFS analysis.

To investigate the effect of Mo impregnation on the surface area and pore volume of the catalyst particles, N₂ physisorption measurements were performed. The blank Al₂O₃ support showed a surface area of 170 m²g⁻¹ (measured by using the BET method^[32]) and a pore volume of 0.46 cm³g⁻¹ (measured by using the BJH method^[33]), whereas for the fresh MoO₃/Al₂O₃ catalyst (4 times impregnated), a BET surface area of 180 m²g⁻¹ and a pore volume of 0.45 cm³g⁻¹ were measured. According to these results, impregnation and calcination of the support change the porous structure only slightly. The impregnation resulted in 9 wt% loading of Mo on the Al₂O₃ support, as measured by using inductively coupled plasma optical emission spectroscopy (ICP–OES).

H₂S removal under dry conditions

In the producer gas from biomass or coal gasification, H₂S is usually the most abundant sulfur species. Therefore, we first investigated H₂S removal under dry conditions. The fresh catalyst was heated to 600 °C and exposed to periodically changing atmosphere, which simulated the conditions in a chemical looping desulfurization reactor. After reduction in 1.25% H₂ for 180 s, 2000 ppm H₂S was added to the total feed of 25 mLmin⁻¹ for 900 s, which corresponded to a total sulfur amount of 33.5 μmol. These conditions represent the reducing conditions for the sulfur-containing producer gas, which usually also contains CO, CO₂, and CH₄. After a purge in He for 60 s,

the catalyst was oxidized in 4% O₂ for 180 s to regenerate the sample. The cycles were repeated 10 times. The selected MS traces for H₂ (detected at *m/z* 2), H₂S and O₂ (both measured at *m/z* 33), and SO₂ (*m/z* 64) of one representative cycle of reduction, sulfidation, and regeneration at 600 °C are shown in Figure 3. Although H₂S is not detected at the reactor outlet

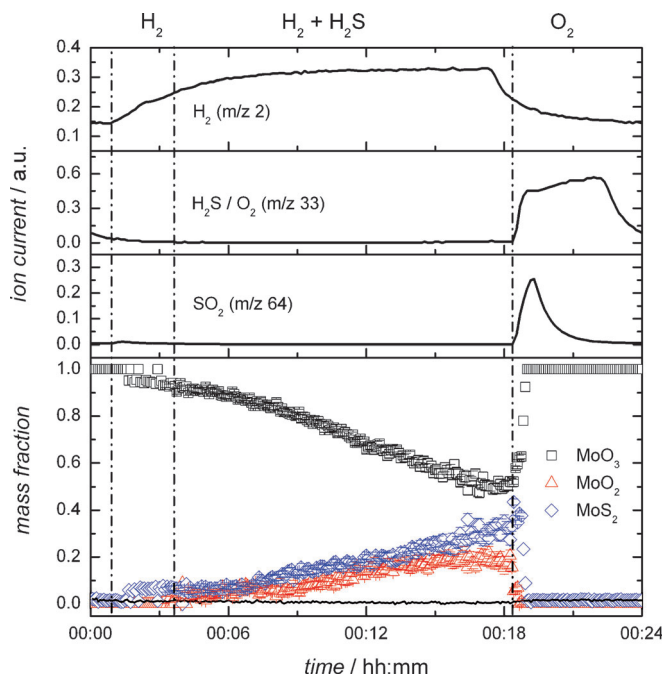


Figure 3. Cyclic exposure of the Mo/Al₂O₃ catalyst to reduction in H₂, sulfidation in H₂ + H₂S, and oxidation in O₂ at 600 °C. The selected MS traces of one cycle for the reactor outlet are shown along with the sample composition, which is derived from the linear combination fit of the Mo K-edge XANES spectra.

during exposure to 2000 ppm H₂S within 900 s, SO₂ is detected upon oxidation with 4% O₂. One measure for the stability of this process is the amount of SO₂ that is generated during each cycle upon oxidation, which is shown in Figure 4 as the integrated signal at *m/z* 64 over 10 cycles. These data suggest that H₂S is effectively removed from the producer gas stream by the Mo/Al₂O₃ catalyst over multiple cycles and oxidized to

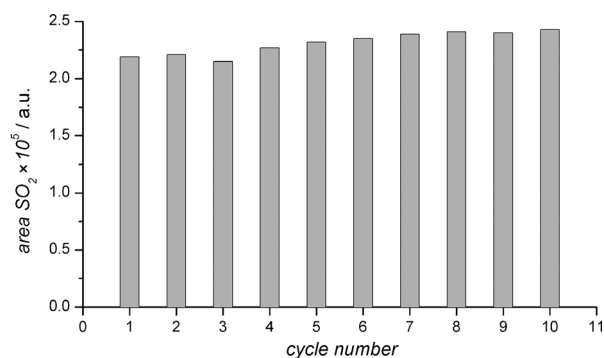


Figure 4. Integrated SO₂ signal (detected at *m/z* 64) over 10 cycles of H₂S exposure to the Mo/Al₂O₃ catalyst at 600 °C.

SO₂. The resulting SO₂ stream can be separated by performing oxidation in a separate reactor, for instance, in a chemical looping reactor or a swing reactor.

To gain insight into the mechanism of sulfur removal by the Mo-based catalyst, time-resolved in situ XAS at the Mo K-edge was used during the cycles of reduction, sulfidation, and oxidation. The XAS spectra were averaged over 10 cycles. Linear combination fitting (LCF) can be used to fit the percentage of known reference states of the catalyst. Applying LCF to time-resolved XAS spectra enables the detection of trends in the reaction. The spectra were fitted with three components: MoO₃, MoO₂, and MoS₂. Here, we used the spectrum of the fresh catalyst (Figure 1) as reference for MoO₃, because the MoO₃ nanoparticles differ slightly in their XANES signals from the MoO₃ reference sample. Linear combination fits of the selected XANES spectra at the beginning of sulfidation in H₂S, during sulfidation, at the end of sulfidation, and after oxidation are shown in Figure 5a. The resulting time-resolved composition

While the XANES region (up to 100 eV above the absorption edge) probes the electronic structure of the sample, the local geometric environment is probed by the EXAFS part of the spectrum. The Fourier transforms of the selected EXAFS spectra during the sulfidation and regeneration cycle are shown in Figure 5b. After oxidation, a single peak at approximately 1.2 Å (not phase corrected) is visible at a position similar to that in the fresh, calcined sample (Figure 1), which indicates full oxidation to MoO₃. Upon exposure to H₂, the intensity of this peak decreases whereas a second peak at approximately 1.7 Å appears. During sulfidation, the peak at 1.2 Å decreases in intensity whereas the peak at 1.7 Å increases in intensity and shifts to higher distances. The Mo–O scattering shell of MoO₃ has the peak at 1.2 Å, whereas Mo–O and Mo–S scattering shells of MoO₂ and MoS₂ have peaks between 1.5 and 2 Å. This result suggests that the fraction of MoO₃ in the sample decreases over time whereas the fractions of MoO₂ and MoS₂ increase. Fitting of the full EXAFS spectra of such mixtures, with many

scattering paths overlapping at similar distances, is not possible with the data quality obtained herein. Nevertheless, the qualitative interpretation of the EXAFS spectra supports the findings of LCF of the XANES spectra in Figure 3.

H₂S removal in the presence of steam

All woody biomass contains moisture, with content varying between 6.5% (for fir) and 60% (for willow).^[22] In addition, steam is often used as a gasification medium.^[34] Thus, the producer gas after biomass gasification contains rather large amounts of steam. Therefore, it is imperative that any high-temperature gas cleaning process operates reliably in the presence of steam, because condensation for steam removal would require cooling,

which is to be avoided. The experiment of reduction, H₂S removal, and oxidation was repeated with additional steam, and the mass of the catalyst in the reactor was varied. The feed rate of H₂O was 0.1 mL h⁻¹, which corresponds to approximately 7.7% steam content at a dry gas flow rate of 25 mL min⁻¹. The integrated H₂S signals at the reactor outlet are shown in Figure 6, which are normalized to the He signal and averaged over 10–15 cycles. For comparison, the integrated signal of the dry experiment is also shown in the figure. Although the presence of steam reduces the H₂S uptake of 25 mg of the catalyst by approximately 40% compared to that under dry conditions, higher amounts of the catalyst lead to complete H₂S removal even in the presence of steam, which indicates that the pres-

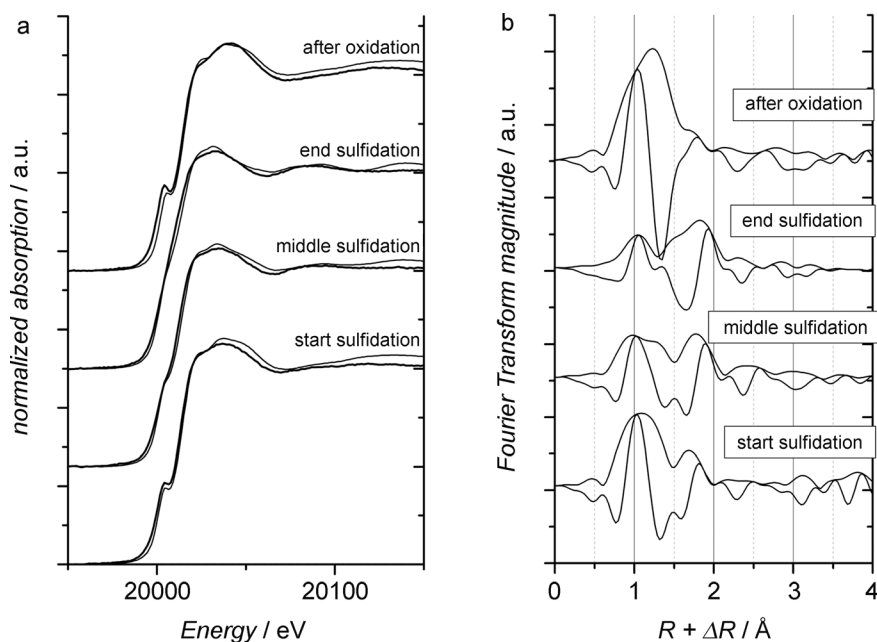


Figure 5. a) XANES spectra (bold lines) with linear combination fits (thin lines) and b) Fourier transforms of the selected spectra after reduction, during sulfidation, after sulfidation, and upon oxidation.

of the Mo catalyst over 1 cycle of sulfidation and oxidation is shown in Figure 3. Exposure to 1.25% H₂ does not substantially reduce the catalyst, and even a small fraction of MoS₂ is determined from linear combination fits. However, upon exposure to 2000 ppm H₂S, MoO₃ is consumed whereas MoO₂ and MoS₂ are formed at a similar rate. At the end of the sulfidation period, approximately 50% of the sample in the X-ray beam is MoO₃, 30% is sulfided to MoS₂, and 20% is MoO₂. The LCF results indicate that the Mo catalyst is fully oxidized to MoO₃ upon exposure to 4% O₂ within a few seconds. The difference between 1 and the sum of the three fractions, that is, the non-fitted fraction, is represented by the black line. The nonfitted fraction never exceeded 2%.

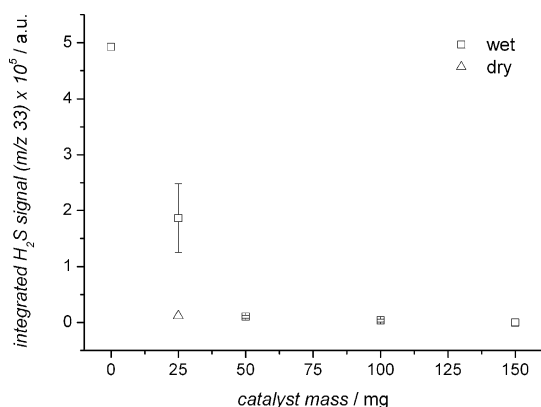


Figure 6. Integrated H_2S signal at the reactor outlet (measured at m/z 33) for different catalyst masses under identical experimental conditions at 600°C with 7.7% steam. The data for a mass of 0 g represent the measurement through an empty tube. For comparison, the data from the dry experiment for a mass of 25 mg are denoted by the blank triangle.

ence of steam reduces H_2S removal but can be compensated for by using a larger amount of the catalyst.

$\text{C}_4\text{H}_4\text{S}$ removal under dry conditions

In the producer gas from gasified biomass, sulfur is present not only as H_2S but also as organic sulfur species, which also need to be removed from the gas stream. As a model compound for organic sulfur species, $\text{C}_4\text{H}_4\text{S}$ was chosen here. Similar to the cyclic sulfidation under H_2S (see above), the catalyst was exposed to periodic reduction, exposure to $\text{H}_2 + \text{C}_4\text{H}_4\text{S}$, and oxidation at a constant temperature of 600°C . In Figure 7, a comparison of the MS data for the reactor inlet (dashed lines) and the reactor outlet (solid lines) shows that all 200 ppm $\text{C}_4\text{H}_4\text{S}$ (m/z 84) that the Mo catalyst is exposed to is removed in the presence of 40% H_2 . Upon oxidation, SO_2 is generated, which indicates that sulfur was bound to $\text{Mo}/\text{Al}_2\text{O}_3$ and oxidized in 4% O_2 . A control experiment with a blank Al_2O_3 support under identical conditions did not show detectable interaction of Al_2O_3 with $\text{C}_4\text{H}_4\text{S}$ (data not shown). The removal of $\text{C}_4\text{H}_4\text{S}$ from the gas stream can therefore be attributed to the Mo particles.

LCF was performed on the time-resolved XANES data of the averaged cycle of reduction, exposure to $\text{H}_2 + \text{C}_4\text{H}_4\text{S}$, and subsequent oxidation. The LCF results illustrated in Figure 7 indicate that MoO_3 readily reduces to approximately 30% MoO_2 and 70% MoO_3 after exposure to 40% H_2 . Compared to the results of the experiment on H_2S uptake (Figure 3), the amount of MoO_2 is higher owing to the higher H_2 concentration. Over the time on stream during exposure to 40% $\text{H}_2 + 200$ ppm $\text{C}_4\text{H}_4\text{S}$, the Mo catalyst fraction slowly reduces further. Upon oxidation in 4% O_2 , Mo is completely oxidized to MoO_3 .

In contrast to the results of the experiment on H_2S uptake, no significant fraction of MoS_2 is found. Within 15 min, the catalyst is exposed to approximately $3.3 \mu\text{mol}$ of $\text{C}_4\text{H}_4\text{S}$. In the experiment with sulfidation by H_2S (see above), approximately 30% of the Mo catalyst in the X-ray beam sulfides to MoS_2 after exposure to $33.5 \mu\text{mol}$ of H_2S . Therefore, exposure to

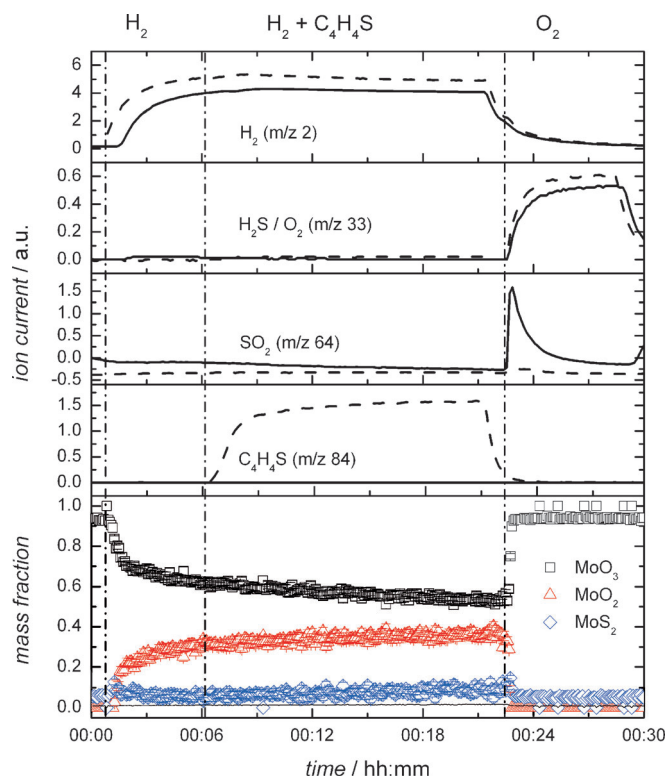


Figure 7. Cyclic exposure of the $\text{Mo}/\text{Al}_2\text{O}_3$ catalyst to reduction in H_2 , reduction in $\text{H}_2 + \text{C}_4\text{H}_4\text{S}$, and oxidation in O_2 at 600°C . The selected MS traces for the reactor inlet (dashed line) and the reactor outlet (solid lines) are shown along with the sample composition (bottom panel), which is derived from the linear combination fit of the Mo K-edge XANES spectra.

$3.3 \mu\text{mol}$ of $\text{C}_4\text{H}_4\text{S}$ is expected to result in approximately 3% of Mo to be present in the MoS_2 phase, which is below the detection limit of the LCF of the XAS spectra (typically 5–10%).

Results from the Fourier-transformed EXAFS spectra, shown in Figure 8, are qualitatively similar to those from LCF. Upon reduction, the intensity of the scattering shell at approximately 1.2 \AA decreases whereas a scattering shell at approximately 1.8 \AA appears. The first peak at 1.2 \AA can be attributed to the first Mo–O coordination shell from MoO_3 , and the scattering shell at 1.8 \AA can be assigned to the first Mo–O coordination shell from MoO_2 (see the reference spectra in Figure 1).

Modulated excitation spectroscopy was shown to enhance the fitting precision of the XAS spectra by filtering out all those parts in the spectrum that do not follow the excitation frequency, which is here the switching of the gas feed.^[35–37] The remaining spectra, called demodulated or phase-detected spectra, are essentially difference spectra between the different states of the catalyst during one excitation cycle but with a better signal-to-noise ratio and only those contributions to the spectra that change upon excitation. Although the XANES or EXAFS data in Figures 7 and 8 provide no conclusive evidence for the formation of MoS_2 , the demodulation of the spectra, which are modulated with the switching of gases, allows sensitive detection of minute changes in the structure of the sample.^[37] The demodulation of the spectra transforms them from the time domain to a phase domain. The selected

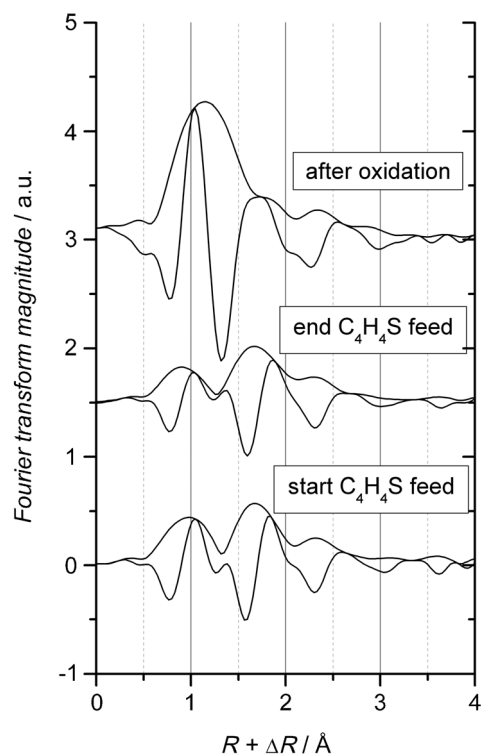


Figure 8. Selected Fourier transforms of the XAS spectra during the cyclic exposure of the Mo/Al₂O₃ catalyst to H₂, H₂ + C₄H₄S, and O₂ at 600 °C.

demodulated spectra are shown in Figure 9 in k space and R space for different phase angles Φ_k . The demodulated spectra in k space show that at least two contributions to the spectra exist, with the major contribution at $\Phi_k=310^\circ$ and the minor contribution at $\Phi_k=223^\circ$. The two spectra demonstrate a distinctly different shape with strong contributions at different k values. The Fourier transformation of the demodulated spectra at $\Phi_k=310$ and 223° in R space shows those scattering shells that change upon excitation, that is, the switching of the gas atmosphere from H₂ to H₂ + C₄H₄S and to O₂. For qualitative comparison, they are plotted along with the difference spectra of reference compounds of MoO₃, MoO₂, and MoS₂. This comparison indicates that the demodulated spectrum at 310° is similar to the difference spectra of MoO₃ and MoO₂ between 1 and 2 Å, which indicates that this spectrum corresponds to the reduction of MoO₃ to MoO₂ of a fraction of the sample. The peak of the demodulated spectrum at 223° at $R \approx 1.7$ Å is in phase with the difference spectra of MoO₂ and MoS₂, which is indicative of the sulfidation of MoO₂ to MoS₂. The amplitude of the demodulated spectrum at 223° is approximately 10 times smaller than that of the spectrum at 310° , which indicates that a much smaller fraction of Mo atoms is sulfided. Thus, the demodulated spectra suggest that the sample transforms from MoO₃ to MoO₂, which is confirmed by the linear combination fit of the XANES spectra. Furthermore, a fraction of the sample is transformed from MoO₂ to MoS₂, which is not readily visible in the XANES or EXAFS spectra.

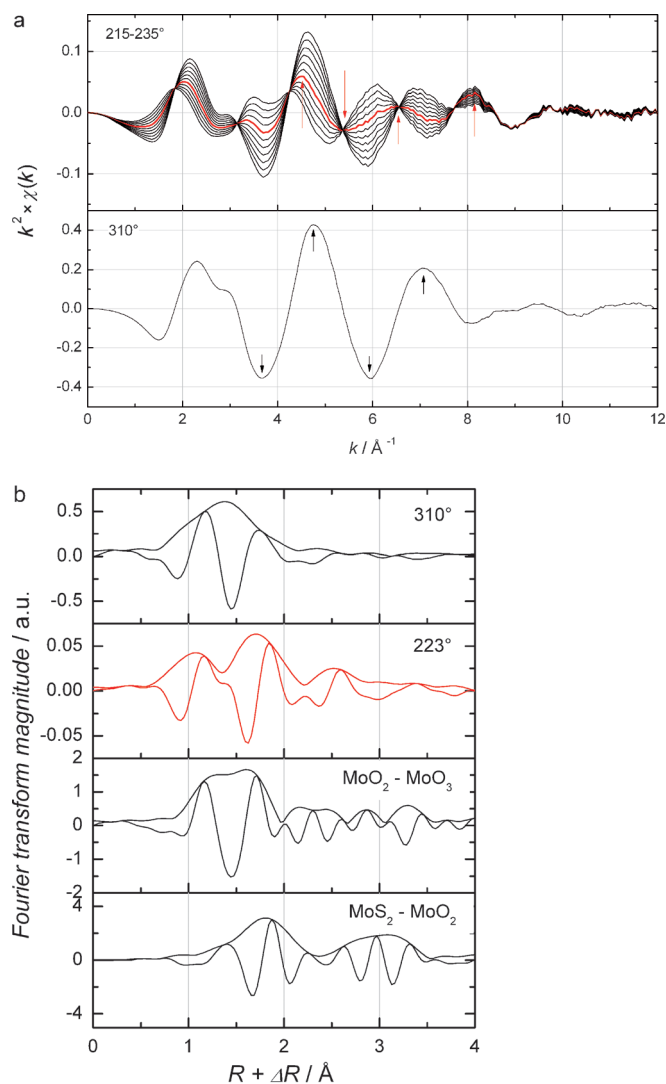


Figure 9. a) Selected demodulated XAS spectra during the cyclic exposure of the Mo/Al₂O₃ catalyst to H₂, H₂ + C₄H₄S, and O₂ at 600 °C. The spectrum at 223° is shown as a thick red line. b) Fourier transforms of the selected demodulated XAS spectra and of the difference spectra of reference compounds.

Effect of prereduction on C₄H₄S removal

In a cyclic process in which the catalyst is exposed to an alternating atmosphere of the sulfur-containing producer gas, which is usually reducing, and oxidizing gas for regeneration, the oxidation state of most of the Mo atoms is changing (Figure 3). To study the effect of the oxidation state of Mo on C₄H₄S removal, the duration of reduction before the addition of C₄H₄S was varied. The C₄H₄S signal detected at the reactor outlet is shown in Figure 10 for different durations of reduction. The removal of C₄H₄S from the gas stream depends on the time of previous reduction. The amount of C₄H₄S that is detected at the reactor outlet decreases over time on stream, which coincides with the progressing reduction of MoO₃ to MoO₂ (Figure 7). For longer times of prereduction, the amount of C₄H₄S that is detected upon the addition of C₄H₄S to the

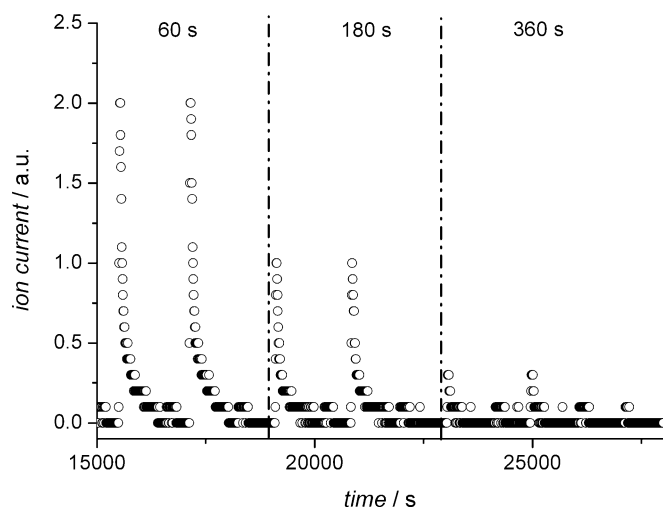


Figure 10. C_4H_4S signal (measured by m/z 84) over time during cyclic reduction, exposure to $H_2 + C_4H_4S$, and oxidation for different times of prereduction.

stream decreases, which suggests that MoO_2 is more favorable for C_4H_4S removal than is MoO_3 .

Effect of H_2 on C_4H_4S removal

Although the removal of C_4H_4S under dry conditions is accomplished in the cyclic process (see above), the aforementioned results do not clarify whether the removal of C_4H_4S is due to pure sorption of C_4H_4S on MoO_2 or whether it is a catalytic process. To study this question, the cycles of reduction, exposure to C_4H_4S , and oxidation were modified and the simultaneous feed of C_4H_4S with H_2 was compared with the feed of C_4H_4S without H_2 . In both cases, the catalyst was reduced in 40% H_2 before the addition of 200 ppm C_4H_4S because, as shown above, a previously reduced catalyst is required for C_4H_4S conversion. If the presence of H_2 affects the removal of C_4H_4S , H_2 must participate in a catalytic process. Otherwise, the removal of C_4H_4S can be described as pure sorption.

The integrated C_4H_4S signal (detected at m/z 84) for the reactor inlet, the reactor outlet with only C_4H_4S in the feed, and simultaneous feed of H_2 and C_4H_4S is shown in Figure 11. As before, all experiments were performed at 600 °C. In the absence of H_2 , approximately 40% of the C_4H_4S fed into the reactor is measured at the outlet; hence, 60% sorbs on the sample. On feeding H_2 simultaneously, no C_4H_4S is detected at the reactor outlet. This result suggests that the removal of C_4H_4S over a prereduced Mo catalyst proceeds at least partially catalytically, most likely owing to the hydrogenation of C_4H_4S to H_2S as well as C_4H_6 and other hydrocarbons. The experiment in the absence of H_2 shows that a fraction of C_4H_4S is removed from the gas stream through sorption on the catalyst.

Effect of sulfidation on C_4H_4S removal

The decomposition of C_4H_4S in the presence of H_2 (see the previous section) will most likely lead to the sulfidation of the Mo

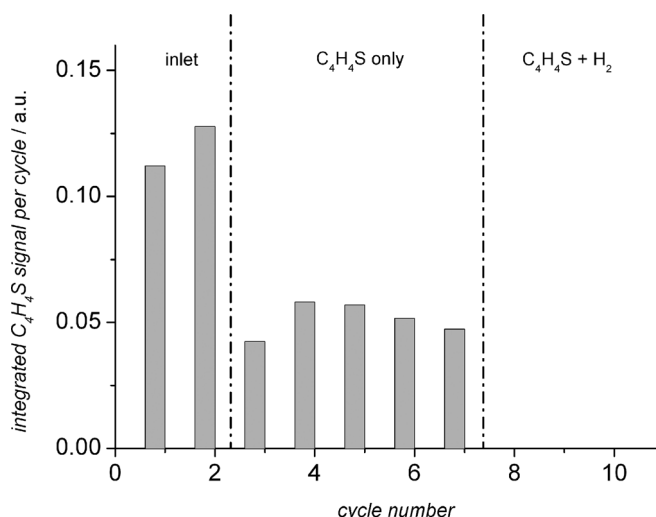


Figure 11. Integrated C_4H_4S signal (measured at m/z 84) at the reactor inlet (cycles 1 and 2) and at the reactor outlet in the absence of H_2 (cycles 3–7) and in the presence of H_2 (cycles 8–10).

catalyst (Figure 9). As the sulfidation of Mo by H_2S (from either the feed or the hydrogenation of C_4H_4S) and C_4H_4S removal occur in parallel, it is important to understand the effect of the sulfidation of the catalyst on C_4H_4S removal. To test this, 50 mg of the Mo/Al_2O_3 catalyst was presulfided before exposure to C_4H_4S . After approximately 220 min of sulfidation at 600 °C in the presence of 40% $H_2 + 1000$ ppm H_2S , the catalyst was exposed to 40% $H_2 + 100$ ppm C_4H_4S at the same temperature. The selected MS traces obtained during sulfidation and subsequent C_4H_4S exposure are shown in Figure 12. After sulfidation, C_4H_4S was removed completely and small amounts of H_2S and C_4H_6 were generated. This finding confirms that a sulfided Mo catalyst is also active for the removal of C_4H_4S from the gas stream as expected because of its use in HDS applications.

Breakthrough of C_4H_4S

For a better understanding of the mechanisms of C_4H_4S removal, a breakthrough experiment was performed under steady-state conditions, and the selected MS traces obtained through that experiment are shown in Figure 13. After reduction in 40% H_2 for 6 min, 25 mg of the catalyst was exposed to 40% H_2 and 100 ppm C_4H_4S at 600 °C at a total gas flow rate of 25 mLmin⁻¹. At the beginning of the exposure, no H_2S (m/z 33) or C_4H_4S (m/z 84) is detected at the reactor outlet, as observed in the previous dry experiments. Approximately 2700 s (45 min) after the start of C_4H_4S exposure, C_4H_4S is detected at the reactor outlet, along with H_2S . During the next 5 h, the signals for C_4H_4S and H_2S rise slowly and reach a steady state eventually. In addition, various C_1 – C_4 species are detected. Before breakthrough of C_4H_4S , the signals for CH_4 (m/z 15), C_2H_4 (m/z 26 and 27), and C_2H_6 (m/z 27 and 30) are detected, along with those for C_4H_8 (m/z 27, 28, and 41) and C_4H_{10} (m/z 27, 28, 41, 42, and 43). At the time when C_4H_4S breaks through, the signals for CH_4 , C_2H_4 , C_2H_6 , and C_4H_{10} reach a maximum. After breakthrough, the signals for CH_4 and C_2H_6 decrease to

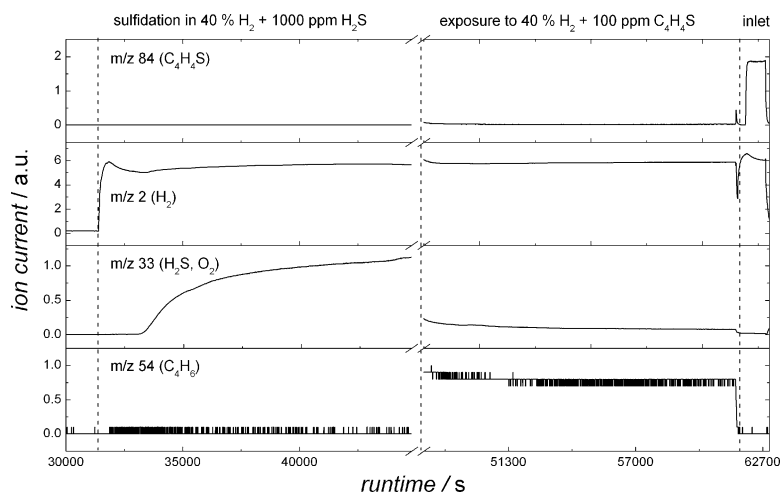


Figure 12. Selected MS traces obtained during the sulfidation and subsequent exposure of the Mo/Al₂O₃ catalyst to H₂ + C₄H₄S at 600 °C.

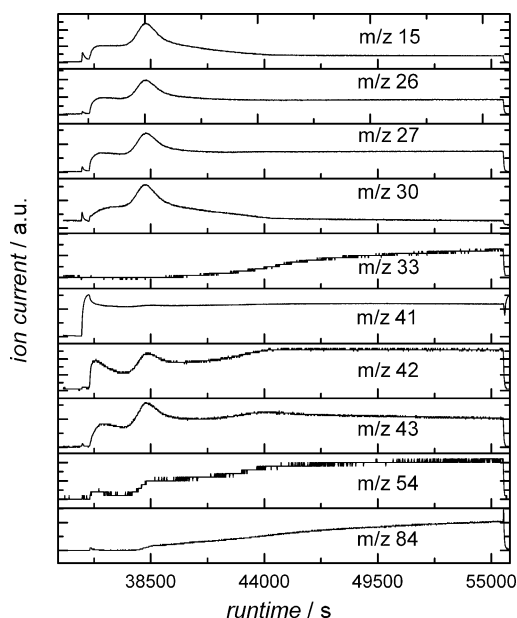


Figure 13. Selected MS traces obtained during the continuous exposure of the Mo/Al₂O₃ catalyst to H₂ + C₄H₄S at 600 °C.

zero, the signals for C₂H₄ and C₄H₁₀ return to near initial levels, and a signal for C₄H₆ (*m/z* 54) is detected.

These data indicate that over the time on stream of continuous exposure to H₂ + C₄H₄S, the selectivity toward carbon conversion changes. In the beginning, some of the carbon rings of C₄H₄S are cracked to C₁ and C₂ species. After C₄H₄S breakthrough, the selectivity shifts toward C₃ and C₄ species. Although the detailed mechanism for the selectivity toward different carbon species is beyond the scope of this study, the results indicate a shift in selectivity that coincides with that in C₄H₄S breakthrough.

C₄H₄S removal in the presence of steam

To assess the effect of steam on the removal of C₄H₄S, the cyclic experiments of reduction, exposure to C₄H₄S, and oxidation (Figure 7) were repeated in the presence of 7.7% steam in the feed. The selected MS traces of one representative cycle are shown in Figure 14. In contrast to the dry experiment, the MS results show only partial conversion of C₄H₄S. Directly after the addition to the gas feed, the C₄H₄S signal detected at the reactor outlet is approximately 60% of the signal detected at the reactor inlet.

The sample composition, determined by the linear combination fit of the time-resolved XAS spectra, suggests no qualitative difference from that in the dry experiment (Figure 7). Upon addition of H₂, approximately 40% of the sample reduces from MoO₃ to MoO₂, which oxidizes quickly to MoO₃

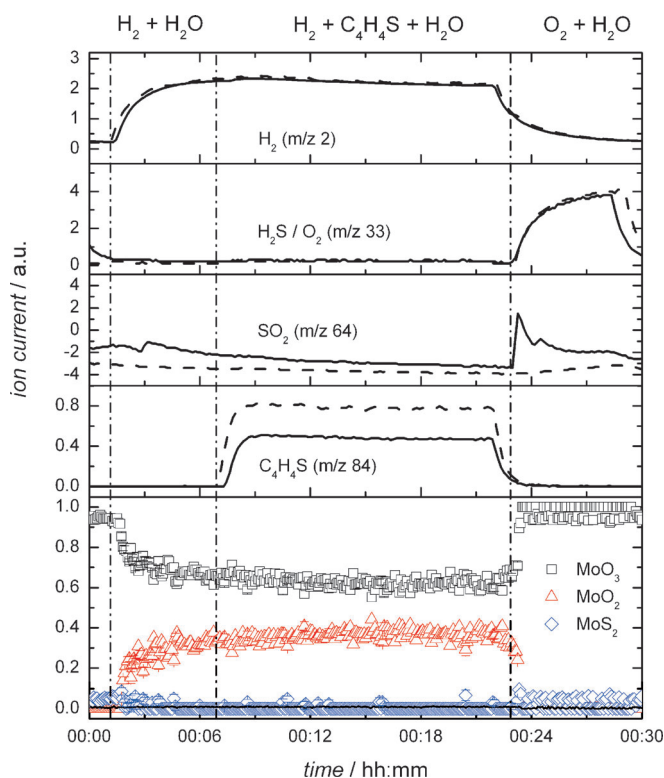


Figure 14. Cyclic exposure of the Mo/Al₂O₃ catalyst to reduction in H₂, reduction in H₂ + C₄H₄S, and oxidation in O₂ at 600 °C in the presence of 7.7% steam. The selected MS traces (top panel) for the reactor inlet (dashed line) and the reactor outlet (solid lines) are shown along with the sample composition, which are derived from the linear combination fit of the Mo K-edge XANES spectra.

upon oxidation in O₂. The degree and speed of reduction and oxidation are not changed significantly upon addition of steam.

Similar to the experiment on H₂S uptake (see above), the amount of catalyst in the reactor was varied whereas all other experimental parameters were kept constant during reduction, exposure to C₄H₄S, and oxidation in the presence of steam. The integrated signal for C₄H₄S at the reactor outlet is shown in Figure 15. The MS data detected at *m/z* 84 (C₄H₄S) was nor-

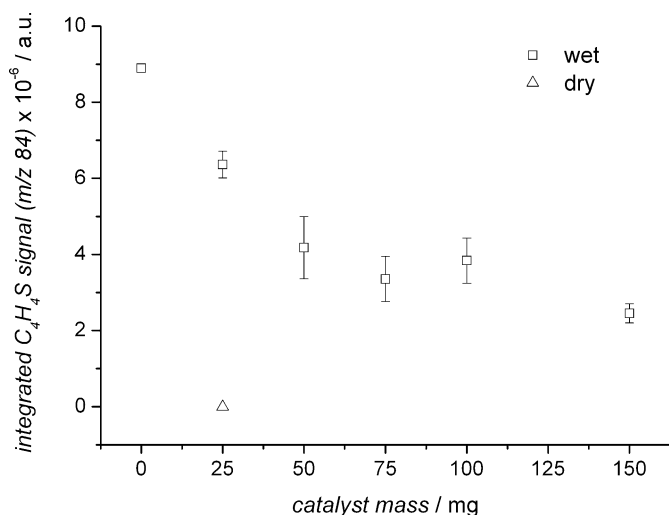


Figure 15. Integrated C₄H₄S signal at the reactor outlet (measured by *m/z* 84) for different catalyst masses under identical experimental conditions at 600 °C in the presence of 7.7% steam. The data for a mass of 0 g represent the measurement through an empty tube. For comparison, the data from the dry experiment for a mass of 25 mg are denoted by a blank triangle.

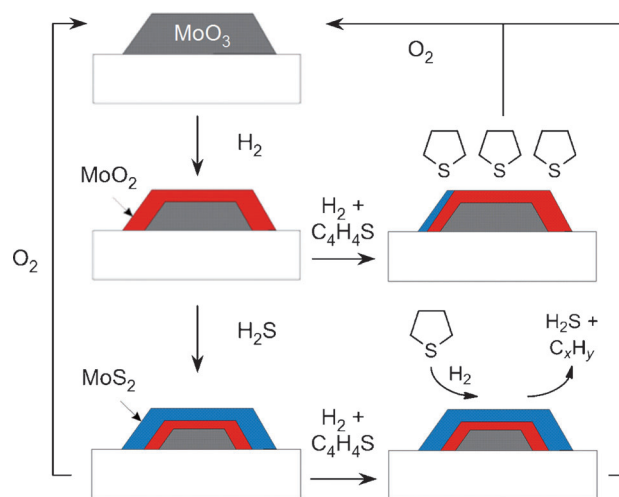
malized to the He signal (*m/z* 4) and integrated over single cycles, and the mean values and standard deviations were calculated for data from 13 to 15 cycles. Although the resulting standard deviations are relatively large, the trend shows that with the increasing catalyst mass a lower C₄H₄S signal is detected at the reactor outlet, which indicates that the detrimental effect of steam is due to the competitive adsorption of H₂O on the MoO₂ surface, blocking sites for C₄H₄S to adsorb. This effect can be compensated for by using more catalyst material. For comparison, the data for 25 mg of the catalyst material from the dry experiment are shown, in which no C₄H₄S is detected at the reactor outlet.

Discussion

Mechanism of sulfur removal

The results for the reactivity (measured by using MS) and structure of the Mo catalyst (measured by using XAS) enable us to propose mechanisms of sulfur removal. These proposed mechanisms of the removal of H₂S and C₄H₄S over Mo are illustrated in Scheme 1 and discussed below.

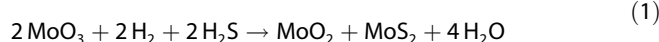
From the experiments on H₂S uptake (Figures 2–4), it can be concluded that the removal of H₂S from the producer gas



Scheme 1. Representation of the mechanisms during H₂S and C₄H₄S removal. ■: MoO₃, ■: MoO₂, ■: MoS₂.

occurs through the sulfidation of MoO₃ to MoS₂ under the concurrent formation of MoO₂. Under oxidizing atmosphere, MoS₂ is oxidized to MoO₃ along with the release of SO₂ [Eqs. (1) and (2)].

Sulfidation :



Regeneration :



This mechanism is in line with earlier findings, which indicated that MoO₃ is sulfidated to MoS₂ via O–S exchange followed by reduction.^[38–41] Temperature-programmed sulfidation experiments showed that MoO₃ supported on Al₂O₃ can be sulfidated at 500 K via O–S exchange on Mo⁶⁺ ions followed by reduction to Mo⁶⁺.^[38] This finding was later supported by X-ray photoelectron spectroscopy (XPS) and IR emission spectroscopy studies on crystalline MoO₃,^[39] by XPS studies on SiO₂-supported MoO₃ model catalysts,^[40] and by XAS and TEM studies on MoO₃/SiO₂ catalysts.^[41]

For the removal of C₄H₄S, a MoO₂ surface is preferred to a MoO₃ surface (Figure 10). The experiments of C₄H₄S removal reveal several plausible mechanisms of the removal:

- 1) C₄H₄S can adsorb on the MoO₂ surface, on which it does not react further, until all possible sites are occupied (sorption).
- 2) C₄H₄S can adsorb on the MoO₂ surface, on which it is hydrogenated by H₂ to H₂S and hydrocarbons, mostly C₄ and only small amounts of C₁–C₃ species (hydrogenolysis).^[42] Subsequently, the generated H₂S reacts with MoO₂ and form MoS₂ and H₂O.
- 3) The adsorbed C₄H₄S can directly sulfide the Mo site on which it adsorbs and forms C₁–C₄ hydrocarbons (direct desulfurization).

In mechanism 1, the only measured species after all Mo sites are occupied would be C_4H_4S . Mechanism 2 would lead to the detection of H_2S and hydrocarbons after breakthrough, whereas mechanism 3 would result in the breakthrough of C_4H_4S and hydrocarbons.

The presented data indicate that the mechanism of C_4H_4S removal is not pure sorption (mechanism 1) of the C_4H_4S molecule on the MoO_2 surface, because H_2 is required to completely remove C_4H_4S from the gas (Figure 11), indicating a catalytic process. The demodulation of the XAS spectra (Figure 9) suggests that a fraction of the catalyst undergoes transition from MoO_2 to MoS_2 during exposure to H_2 and C_4H_4S .

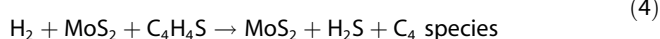
The breakthrough of C_4H_4S with some production of H_2S indicates that hydrogenolysis is not the prevailing mechanism of C_4H_4S removal over MoO_2 . If that was the case, as it is for pre-sulfided Mo (Figure 12), only H_2S would be observed in the breakthrough experiment, but no C_4H_4S .

Thus, C_4H_4S is removed from MoO_2 mainly through the direct desulfurization of C_4H_4S . Sulfur-free surfaces are covered initially with C_4H_4S , which completely removes C_4H_4S from the gas. In the presence of H_2 , the adsorbed C_4H_4S then sulfides MoO_2 whereas hydrocarbons are released. The observation of CH_4 in this initial phase indicates that the carbon structure is completely cracked to C_1 species, possibly owing to the presence of acid sites on MoO_2 .^[43] This process occurs at a rate slower than the feed rate of C_4H_4S , which leads to the observed breakthrough of C_4H_4S [Eqs. (3) and (4)].

Direct desulfurization :



Hydrogenolysis :



The MoS_2 phase formed through sulfidation in H_2S is active for the removal of C_4H_4S in the presence of H_2 (Figure 12), which forms C_4H_6 and H_2S .

As the Mo catalyst removes H_2S through sorption and subsequent sulfidation and C_4H_4S through a catalyzed reaction, we consider it a bifunctional material. In this context, bifunctionality is defined as the capability of the material to remove sulfur from the gas stream through two mechanisms: sorption and catalysis.

The direct mechanistic insight that is presented in this contribution is possible only owing to the use of time-resolved in situ XAS. Although in situ studies using other techniques will suffer from small particle size (not possible using XRD), large amounts of steam (not possible using IR spectroscopy), or ambient pressure (not possible using XPS), XAS is a tool that is complementary to the routinely used gas analysis. Although gas analysis provides direct information only on the catalyst activity, its structure can be directly observed by using XAS.

Effect of steam

Steam, which is always present in the producer gas from gasified biomass, has a detrimental effect on the desulfurization over Mo/Al_2O_3 catalysts. However, the reduction/oxidation of Mo is not significantly affected by the presence of steam (Figures 6 and 7), which is in line with the findings from ex situ experiments using XPS.^[23] In contrast, it seems that H_2O adsorbs competitively on the surface to H_2S and C_4H_4S , which in effect slows down the desulfurization reactions. Although the decreased activity can be compensated for by using more catalyst material, the activity in a real system will depend on the process parameters (temperature, steam content, etc.) and the catalyst formulation (Mo loading, dispersion, addition of promoters, etc.).

Suitability of Mo catalysts for hot gas desulfurization

The presented results indicate that Mo/Al_2O_3 is a suitable catalyst for hot gas desulfurization. At $600^\circ C$, H_2S and C_4H_4S , which are used here as model compounds for sulfur species in the producer gas, are removed under dry conditions. Over the 10–15 cycles under a reducing and oxidizing atmosphere, the catalyst is stable, as indicated by the stable levels of SO_2 , which is removed upon oxidation (see Figure 4), enabling long-term use for desulfurization. The adjustment of the residence time of the catalyst in the sulfur-containing producer gas will avoid the breakthrough of C_4H_4S . In a real-size plant, the desulfurization over the Mo catalyst is likely to be implemented after a high-temperature filtration step to avoid interaction of the particulate matter with the catalyst.

The promotion of the catalyst with other metals, such as Co, can be an option to minimize the negative effect of steam. A comparison of the unpromoted Mo/Al_2O_3 catalyst with $CoMo/Al_2O_3$ catalysts showed that the former was more prone to the inhibition of hydrodeoxygenation by steam than the latter.^[25] In contrast, promotion with Ni was found to enhance the negative effect of steam owing to the oxidation of nickel sulfides.^[24] Therefore, the development of the dedicated materials for the improved desulfurization of the producer gas must take the effect of H_2O into account.

Conclusions

The suitability of Mo catalysts supported on Al_2O_3 for a hot-gas removal of sulfur in the absence and presence of steam was investigated. Although the activity for sulfur removal was studied by using MS, the state of Mo was probed by using time-resolved in situ X-ray absorption spectroscopy at the Mo K-edge. Experiments at $600^\circ C$ showed that under dry conditions, H_2S , which is the most abundant sulfur species in the producer gas, and C_4H_4S , which is used as a model compound for organic sulfur species, are completely removed by Mo. The presence of steam is detrimental for the removal of H_2S and C_4H_4S from the gas owing to the competitive adsorption of steam on the Mo surface, which blocks sites for sulfur adsorption.

The mechanisms of sulfur removal were proposed on the basis of the measurements of reactivity and structure of the Mo catalyst; H₂S is removed through the sulfidation of MoO₃ to MoS₂ with the concurrent reduction of MoO₃ to MoO₂. The removal of C₄H₄S occurs over MoO₂ through the hydrogenolysis of C₄H₄S, which forms MoS₂ and C₁–C₄ species. This process is, however, slower than the catalytic hydrogenation of C₄H₄S over MoS₂. Subsequent oxidation to SO₂ enables the sequestration of sulfur from the producer gas stream and regeneration of the catalyst.

Herein, we showed that Mo-based catalysts can be used for sulfur removal from biomass-derived gas at high temperatures, which removes H₂S and organic sulfur compounds. This process improves the efficiency of catalytic biomass conversion.

Experimental Section

Materials

The materials were prepared through repeated wetness impregnation. Ammonium heptamolybdate tetrahydrate [(NH₄)₆Mo₇O₂₄·4H₂O, Sigma–Aldrich] was dissolved in deionized water and impregnated on the γ-Al₂O₃ support (Sasol). Excess water was evaporated slowly under vacuum, and the impregnated support was washed with deionized water. Finally, the catalyst was dried at 110 °C for 1 h and calcined at 600 °C for 6 h. This process was repeated 4 times to increase the Mo loading. The sample (≈25 mg) was used for the in situ experiments with H₂S and C₄H₄S. Reference compounds MoO₂, MoO₃, and MoS₂ were purchased from Sigma–Aldrich, diluted in cellulose, and pressed into pellets. Samples were characterized by N₂ physisorption (Micromeritics TriStar II), XRD (Bruker D8), ICP–OES (Varian Vista Pro AX), and STEM. STEM was performed on a Hitachi HD2700C STEM microscope.

Experimental setup

The reactor for the in situ experiments consisted of a quartz capillary (3 mm outer diameter and 0.1 mm wall thickness; Hilgenberg) that was heated by a hot air blower (Leister). The samples were fitted in the reactor between two plugs of quartz wool. The temperature inside the capillary was measured with a thermocouple placed downstream of the bed and was kept at 600 °C. The pressure inside the reactor was kept constant at 0.5 bar overpressure with pressure regulating valves (Bronkhorst). A computer-controlled setup was used to mix gases with mass flow controllers (Bronkhorst). All gas lines were coated with amorphous SiO₂ to minimize sulfur adsorption (Sulfinert, Restek). Gas analysis was performed with a quadrupole mass spectrometer (Max 300-LG, Extrel). Deionized water was injected into the gas stream with a syringe pump (Harvard apparatus) through a fused silica capillary into a crosspiece in a heated box. As this method has limited dynamics of starting and stopping the water feed, steam flow was constant during the experiments with steam. The transfer lines between the crosspiece, the reactor, and the mass spectrometer were heated to avoid condensation.

Setup for XAS

The in situ XAS experiments at the Mo K-edge (20.0 keV) were performed in the transmission mode at the SuperXAS beamline at the

Swiss Light Source using a QuickXAS monochromator with a channel-cut Si (111) crystal that was rotated at a frequency of 0.2 Hz, which resulted in 5 s time resolution per spectrum. The X-ray energy was calibrated with use of a Mo metal foil placed downstream of the sample. The beam intensity was monitored with ion chambers filled with N₂ (*I*₀, before the sample) and Ar (*I*₁ and *I*₂, after the sample and the reference foil, respectively). The X-ray beam was collimated by a Pt-coated mirror upstream of the monochromator and was focused to approximately 100 μm² with a Pt-coated toroidal mirror placed downstream of the monochromator. The ion chamber signals were amplified, the angular encoder signal from the monochromator was converted to analog voltage, and all signals were sampled by an analog-to-digital converter at 1 kHz. The resulting data were averaged over multiple cycles, and the encoder signal was converted into an energy scale with custom MATLAB scripts. Normalization, energy calibration, LCF, and EXAFS fitting were performed with IFEFFIT.^[44] The EXAFS fitting of the fresh catalyst sample was performed over a *k* range of 3–14 Å⁻¹ in *k*² weighting. The value for the amplitude reduction factor (*S*₀²), 0.87, was derived by fitting a spectrum of the Mo foil, which was acquired under identical experimental conditions. LCF was performed over a range of –20 to +50 eV, which was relative to the absorption edge. All components used the same energy shift *E*₀ and were forced to have a weight between 0 and 1. Summing of the components to 1 was not enforced.

Acknowledgements

We thank F. Krumeich and D. Fodor from ETH Zürich for STEM measurements, S. Köchli for ICP–OES analysis, M. Steib for assistance during beamtime, E. de Boni for technical assistance, the Swiss Light Source for providing beamtime. C.F.J.K. acknowledges the Competence Center for Energy and Mobility for funding.

Keywords: biomass · desulfurization · in situ spectroscopy · molybdenum · X-ray absorption spectroscopy

- [1] A. V. Bridgwater, *Appl. Catal. A* **1994**, *116*, 5–47.
- [2] H. de Lasa, E. Salaices, J. Mazumder, R. Lucky, *Chem. Rev.* **2011**, *111*, 5404–5433.
- [3] A. van der Drift, J. van Doorn, J. W. Vermeulen, *Biomass Bioenergy* **2001**, *20*, 45–56.
- [4] W. Torres, S. S. Pansare, J. G. Goodwin, *Catal. Rev.* **2007**, *49*, 407–456.
- [5] H. Cui, S. Q. Turn, V. Keffer, D. Evans, T. Tran, M. Foley, *Energy Fuels* **2010**, *24*, 1222–1233.
- [6] K. Natesan, *Corrosion* **1985**, *41*, 646–655.
- [7] S. Mrowec, *Oxid. Met.* **1995**, *44*, 177–209.
- [8] P. K. Agrawal, J. R. Katzer, W. H. Manogue, *J. Catal.* **1982**, *74*, 332–342.
- [9] W. D. Fitzharris, J. R. Katzer, W. H. Manogue, *J. Catal.* **1982**, *76*, 369–384.
- [10] J. Hepola, P. Simell, *Appl. Catal. B* **1997**, *14*, 305–321.
- [11] K. Okabe, K. Murata, M. Nakanishi, T. Ogi, M. Nurunnabi, Y. Liu, *Catal. Lett.* **2009**, *128*, 171–176.
- [12] S. D. Phillips, *Ind. Eng. Chem. Res.* **2007**, *46*, 8887–8897.
- [13] M. M. Yung, W. S. Jablonski, K. A. Magrini-Bair, *Energy Fuels* **2009**, *23*, 1874–1887.
- [14] K. Engvall, H. Kusar, K. Sjoestroemm, L. J. Pettersson, *Top. Catal.* **2011**, *54*, 949–959.
- [15] R. D. Solunke, G. Vesper, *Fuel* **2011**, *90*, 608–617.
- [16] R. K. Srivastava, W. Jozewicz, C. Singer, *Environ. Prog.* **2001**, *20*, 219–228.
- [17] Y. Mathieu, L. Tzanis, M. Souldard, J. Patarin, M. Vierling, M. Molière, *Fuel Process. Technol.* **2013**, *114*, 81–100.
- [18] J. H. Swisher, J. Yang, R. Gupta, *Ind. Eng. Chem. Res.* **1995**, *34*, 4463–4471.

- [19] S. Cheah, D. L. Carpenter, K. A. Magrini-Bair, *Energy Fuels* **2009**, *23*, 5291–5307.
- [20] X. Meng, W. de Jong, R. Pal, A. H. M. Verkooijen, *Fuel Process. Technol.* **2010**, *91*, 964–981.
- [21] H. Topsøe, B. S. Clausen, F. E. Massoth *Catalysis, Science and Technology*, Springer, Berlin, **1996**, p. 1–269.
- [22] P. McKendry, *Bioresour. Technol.* **2002**, *83*, 37–46.
- [23] T. A. Patterson, J. C. Carver, D. E. Leyden, D. M. Hercules, *J. Phys. Chem.* **1976**, *80*, 1700–1708.
- [24] E. Laurent, B. Delmon, *J. Catal.* **1994**, *146*, 281–291.
- [25] M. Badawi, J. F. Paul, S. Cristol, E. Payen, Y. Romero, F. Richard, S. Brunet, D. Lambert, X. Portier, A. Popov, E. Kondratieva, J. M. Goupil, J. El Fallah, J. P. Gilson, L. Mariey, A. Travert, F. Mauge, *J. Catal.* **2011**, *282*, 155–164.
- [26] I. I. Novochinskii, C. Song, X. Ma, X. Liu, L. Shore, J. Lampert, R. J. Farrauto, *Energy Fuels* **2004**, *18*, 576–583.
- [27] R. Prins, V. H. J. de Beer, G. A. Somorjai, *Catal. Rev. Sci. Eng.* **1989**, *31*, 1–41.
- [28] P. T. Vasudevan, L. G. Fierro, *Catal. Rev. Sci. Eng.* **1996**, *38*, 161–188.
- [29] H. Topsøe, B. S. Clausen, *Catal. Rev. Sci. Eng.* **1984**, *26*, 395–420.
- [30] T. Ressler, J. Wienold, R. E. Jentoft, T. Neisius, M. M. Guenter, *Top. Catal.* **2002**, *18*, 45–52.
- [31] E. M. McCarron, J. C. Calabrese, *J. Solid State Chem.* **1991**, *91*, 121–125.
- [32] S. Brunauer, P. H. Emmett, E. Teller, *J. Am. Chem. Soc.* **1938**, *60*, 309–319.
- [33] E. P. Barrett, L. G. Joyner, P. P. Halenda, *J. Am. Chem. Soc.* **1951**, *73*, 373–380.
- [34] T. Gröbl, H. Walter, M. Haider, *Appl. Energy* **2012**, *97*, 451–461.
- [35] D. Ferri, M. S. Kumar, A. Eyssler, O. Korsak, P. Hug, A. Weidenkaff, M. A. Newton, *Phys. Chem. Chem. Phys.* **2010**, *12*, 5634–5646.
- [36] D. Ferri, M. A. Newton, M. Nachtegaal, *Top. Catal.* **2011**, *54*, 1070–1078.
- [37] C. F. J. König, J. A. van Bokhoven, T. J. Schildhauer, M. Nachtegaal, *J. Phys. Chem. C* **2012**, *116*, 19857–19866.
- [38] P. Arnoldy, J. A. M. van der Heijkant, G. D. de Bok, J. A. Moulijn, *J. Catal.* **1985**, *92*, 35–55.
- [39] Th. Weber, J. C. Muijsers, J. H. M. C. van Wolput, C. P. J. Verhagen, J. W. Niemantsverdriet, *J. Phys. Chem.* **1996**, *100*, 14144–14150.
- [40] J. C. Muijsers, Th. Weber, R. M. van Hardeveld, H. W. Zandbergen, J. W. Niemantsverdriet, *J. Catal.* **1995**, *157*, 698–705.
- [41] A. J. de Boer, van Dillen, D. C. Koningsberger, J. W. Geus, *J. Phys. Chem.* **1994**, *98*, 7862–7870.
- [42] D. L. Sullivan, J. G. Ekerdt, *J. Catal.* **1997**, *172*, 64–75.
- [43] N. Sotani, M. Hasegawa, *Bull. Chem. Soc. Jpn.* **1973**, *46*, 25–29.
- [44] M. Newville, *J. Synchrotron Radiat.* **2001**, *8*, 322–324.

Received: March 14, 2013

Published online on September 9, 2013

Copyright of ChemCatChem is the property of Wiley-Blackwell and its content may not be copied or emailed to multiple sites or posted to a listserv without the copyright holder's express written permission. However, users may print, download, or email articles for individual use.